Plane Stress Elastic–Plastic Fracture Criterion and Stress–Strain Field Around Crack Tip

DENG HAITAO and WANG TZUCHIANG
Institute of Mechanics, Academia Sinica, Beijing 100080, PRC

ABSTRACT

In this paper, both experimental and finite element methods have been used to study thin plate elastic-plastic fracture criterion. A stable crack growth experiment was conducted on the center-cracked panels made of 2Cr13 stainless steel under displacement control. The behaviour of crack growth initiation has been modelled by plane stress elastic-plastic (incremental and small strain) finite element analysis in which the critical values of J-integral, crack opening displacement and the strain ahead of crack tip at crack growth initiation were calculated and compared in detail. Plane stress elastic-plastic stress-strain field around crack tip has been calculated for different geometry configuration specimens of strain hardening materials, and then the finite element results of center-cracked panel (CCP), compact tension specimen (CTS) and cracked bend bar (CBB) were discussed and compared with HRR solutions.

KEYWORDS

Elastic-plastic fracture; thin plate fracture criterion; crack tip field; J-integral; HRR singular field.

INTRODUCTION

It has been shown by numerous experiments that the fracture failure problems of some metals exhibit slow crack propagation behaviour. The fracture process from initial loading to failure can be divided into three stages: no crack growth, stable crack growth and unstable crack growth under load control (or stable crack growth with decreasing loading under displacement control). In the past decades, to establish the proper fracture criterion for crack growth initiation and unstable crack failure has been and is still one of the most important objectives in the study of elastic-plastic fracture mechanics.

The J-integral (Rice, 1968) and HRR singular field proposed by Hutchinson (1968), Rice

and Rosengren (1968) provided the theoretical foundation for the J-integral criterion and have had great influence on the development of elastic-plastic tic fracture mechanics. The HRR theory showed that the elastic-plastic stress-strain field near crack tip is dominated uniquely by J-integral for the same material and therefore J-integral may be employed as a fracture criterion for elastic-plastic crack growth initiation. Afterwards, Begley and Landes (1972), Broberg (1971) independently proposed that the J-integral could be used as a fracture criterion if some required size conditions are satisfied. But later investigations by Shih *et al* (1979) have shown significant difference of critical J-integral values at crack growth initiation. The results of finite element calculations using small strain and finite deformation theory indicated that the HRR singular field is valid for the specimens subjected to bend loading such as cracked bend bar (CBB) and compact tension specimen (CTS), but different from the numerical results of tension loading specimens such as center-cracked panel (CCP). Recently, Li and Wang (1986) have suggested a theoretical basis for the double parameter fracture criterion. For plane stress elastic-plastic fracture problems, Liu and Zhuang (1984) have pointed out that the HRR theory is valid compared with finite element results for various the of cracked specimens (CCP, CTS and CBB).

This paper is concerned with the experimental and finite element analysis of thin plate crack growth initiation and propagation. The J-integral, crack opening displacement COD and strain ahead of crack tip at crack growth initiation has been investigated in detail to study elastic-plastic fracture criterion. The stress-strain field has been calculate and compared with the solutions of HRR theory.

CRACK GROWTH EXPERIMENT

The material used in the experiment is 2Cr13 stainless steel. Its chemical composition is given as follows: C, 0.16-0.24; Si, $\leq$0.6; Mn, $\leq$0.8; S, $\leq$0.03; P, $\leq$0.035; Cr, 12-14(%). The stress-strain curve is shown in Figure 1. The mechanical properties of the material are as follows: yielding stress $\sigma_0 = 32.3Kg/mm^2$; maximum stress $\sigma_{max} = 59.8Kg/mm^2$. The geometry size of the center-cracked panel is shown in Figure 2, where $2a_0$is the initial crack length and W the panel width. The crack on test specimens were at first cut out by machining, and then fatigue pre-cracked.

The experiment was conducted under displacement control on MTS hydraulic testing machine. A moire strain gauge of eight lines per millimeter was placed on one side of the center-cracked panel to measure the strain field around crack tip, and on the other side of the panel a 30-80 amplifying coefficient travelling microscope was used to measure the crack length and observe the fracture behaviour at crack growth initiation and during crack propagation process. Five 1.00 mm thickness center-cracked panel with different crack length were tested under the same experiment procedure. The crack lengths of five specimens are 2.74mm, 7.30mm, 9.54mm, 12.02mm and 14.98mm respectively.

FINITE ELEMENT ANALYSIS

An elastic-plastic finite element programme based on small strain incremental plastic-

ity theory was used in modelling crack growth initiation and calculating stress-strain field around crack tip. Von-Mises criterion was employed to predict yielding, and two-dimensional eight-nodded isoparametric element with 9 Gauss points was adapted in the finite element calculations.

The finite element mesh used to model crack growth initiation of center- cracked panel is shown in Figure 3, which contains about 353 nodes and 102 elements. Due to the geometry bend loading symmetry, only one quarter of the panel was calculated. The mesh for the test specimens with different crack length should be changed slightly, and this modification can be completed easily by the automatic mesh creating programme. The length of the element side connected to crack tip is about 0.01 of the panel width.

The stress-strain curve for 2Cr13 stainless steel was presented by a 25-piece linear approximation, which gave a very close fit to the experimental curve (Figure 1).

In order to study the stress-strain field around crack tip, another type of calculation was carried out on center-cracked panel (CCP), compact tension specimen (CTS) and cracked bend bar (CBB) in plane stress case, and for both low and high strain hardening materials. The stress-strain curve was modelled by a power-law relationship in the form of

$$\epsilon/\epsilon_0 = \alpha(\sigma/\sigma_0)^n$$

where σ_0 is the yield stress, ϵ_0 the yield strain, α the strain hardening coefficient and n the hardening exponent. In the calculations, α=1, $\epsilon_0 = 0.002$, $\nu(Poisson's ratio) = 0.3$, E(Young modulus)/$\sigma_0 = 300$.

The typical meshes are shown in Figure 4, which are only one quarter of the specimen of CCP, CTS and CBB due to symmetry. The total mesh contains 114 elements, 393 nodes in Figure 4. The length of the element at crack tip is 0.001 of the length of ligament.

RESULTS AND DISCUSSIONS

Experimental results

The experimental results are presented in Table 1.
where

$2a_0$ —— Initial crack length
$2a_c$ —— Crack length at maximum load.
W —— Specimen width of the center-cracked panel.
P_0 —— Load at crack growth initiation.
P_{max} —— Maximum load.

The results show large scale plastic zones exist on test panels at crack growth initiation. The average stress or the ligament of the specimen is much larger than yield stress of the material when crack begins to extend, especially for short crack panels. It is clearly observed by microscope during the experiment that crack tip exhibits significant blunting phenomenon prior to crack growth initiation regardless of the specimens with

short of long cracks, and the crack tip blunting process may repeat several times before the crack growth initiation. It is necessary to give or suppose an appropriate definition for crack initiation in the crack growth experiment. In this paper, it is assumed that crack initiation occurs when a non-blunting crack growth begins, and therefore the crack growth initiation load P_i can be easily determined.

Figure 5 gives the gauge strain of different gauge length during crack extension, in which $\Delta a = a - a_0$ is the amount of crack extension measured from one side of crack tips, and ϵ_{40},ϵ_{60} and ϵ_{80} are the gauge strains with gauge length of 40mm, 60mm and 80mm.

Observation in the experiment showed that the crack opening angle (COA) essentially remains constant of about 20° during stable crack propagation process, as predicted by H. Andersson (1973).

Crack growth initiation criterion

Table 2 presents the critical values of J-integral, crack opening displacement (COD) and strain ahead of crack tip at crack growth initiation calculated by finite element analysis. It can be seen that J- integral is essentially identical for different crack length panels at crack growth initiation, but it seems the critical values of J-integral changes proportionally to the crack length in a slight amount. Similar conclusions can be drawn by comparing COD and strain results. Crack opening displacement (COD) at a specified distance from the crack tip appears to be a more realistic criterion of crack growth initiation such as the COD with distance of 0.1mm to the crack tip. COD are clearly showed in Figure 6, which gives the crack tip shapes of four specimens at crack growth initiation.

Stress-strain field around crack tip

For high strain hardening material of n=3, stress σ_{yy} distribution ahead of crack tip is shown in Figure 7 from the state of small plastic zone to large plastic region((a) and (b)). The stress is normalized by yield stress σ_0 and the distance from crack tip r is normalized by J/σ_0. It is clear that the finite element results agree very well with the HRR solutions, and this means that the plane stress elastic-plastic stress-strain field around crack tip is independent of the geometry configurations of crack specimens. HRR theory is valid in characterizing crack tip field and therefore a critical value of J-integral can be considered as a satisfied fracture criterion in plane stress case.

Figure 8(a,b) present the stress distribution along the ligament in the same way as Figure 7 for low hardening material of n=10, and also the HRR singular field is almost the same to the finite element results of CCP, CTS and CBB configurations.

CONCLUSIONS

1. For elastic-plastic fracture problems in plane stress case, J-integral can be employed as a crack growth initiation criterion which is independent of the geometry size and

configuration of specimens.

2. Crack opening displacement at specified distance to the crack tip and strain ahead of crack tip are also promising to be elastic-plastic fracture criterion in plane stress case.

3. The finite element results of the crack tip field for the thin plate specimens of CCP, CTS and CBB configurations are identical to each other, and agree well to the HRR solutions.

4. During thin plate stable crack growth process, crack opening angle (COA) essentially remains constant before crack failure.

REFERENCES

J.R.Rice (1968). A Path Independent Integral and the Approximate Analysis of Strain Concentrations by Notches and Cracks. Tran of ASME, J. of Applied Mech., Vol.35, 379-386

J.W.Hutchinson (1968). Singular Behavior at the End of a Tensile Crack in a Hardening Material. J. Mech. Phy. Solids, Vol.16, 13-31

J.R.Rice and G.R.Rosengren (1968). Plane Strain Deformation near a Crack tip in a Power-law Hardening Material. J. Mech. Phy. Solids, Vol.16, 1-12

J.A.Begley and J.D.Landes (1972). The J-Integral as a Fracture Criterion in Fracture Toughness Testing. Fracture Toughness, ASTM STP 514, 1-39

K.B.Broberg (1971). J.Mech.Phys. Solids, Vol.19, 407-418

C.F.Shih, H.G.Delorenzi and W.R.Andrews (1979). Studies on Crack Initiation and Stable Crack Growth. Elastic-plastic Fracture, ASTM STP 668, 65-120

C.F.Shih and M.D.German (1981). Requirements for a One Parameter Characterization of Crack Tip Fields by the HRR Singularity. Inter. J. Fracture, Vol.17, 27-43

R.M.McMeeking and D.M.Parks (1979). On Criteria for J-Dominance of Crack Tip Fields in Large Scale Yielding. Elastic-plastic Fracture, ASTM STP 668, 175-194

A.Needleman and V.Tvergaard (1983). Elastic-plastic Fracture, ASTM STP 803, I-80 - I-115

Wang Tzuchiang (1983). Elastic-Plastic Analysis of Stress and Strain Fields Around Crack tip. Proceedings of ICF International Symposium on Fracture Mechanics, 243-250 (Beijing)

Li Yaochen and Wang Tzuchiang (1986). High-Order Asymptotic Field of Tensile Plane-Strain Nonlinear Crack Problems. Scientia Sinica (Series A), Vol.29, 941-955.

H.W.Liu and Tao Zhuang (1984). Advances in Fracture Research, ICF6, Vol.2, 777-790

H. Andersson (1973). A Finite Element Representation of Stable Crack Growth . J. Mech. Phys. Solids, Vol.21, 337-356.

Table 1: Experimental Results

Panel No.	1	3	5	6	9
$2a_o(mm)$	2.74	9.54	12.02	14.98	7.30
$2a_c(mm)$	8.70	13.64	21.08	21.92	11.64
$W(mm)$	90.32	90.48	95.70	90.50	90.07
$2a_o/W$	0.030	0.105	0.126	0.166	0.081
$P_i(Kg)$	4591	3590	3710	3290	3800
$P_{max}(Kg)$	4659	3802	4386	3961	4160

Table 2: Finite Element Results

Panel No.	3	5	6	9
$2a_o(mm)$	9.54	12.02	14.98	7.30
$P_i(Kg)$	3590	3710	3290	3800
$J_i^*(Kg/mm)$	22.4	24.9	26.7	23.6
$\delta^*_{0.1}(mm)$	0.398	0.417	0.417	0.405
$\delta^*_{0.05}(mm)$	0.325	0.313	0.319	0.333
$\delta_t^\dagger(mm)$	0.436	0.502	0.544	0.470
$\epsilon^\ddagger_{y0.1}$	0.141	0.161	0.168	0.145
$\epsilon^\ddagger_{y0.25}$	0.111	0.131	0.137	0.114

* J-integral at crack growth initiation.
* COD at specified distance of 0.10 and 0.05mm to crack tip.
† COD suggested by Rice.
‡ Strain ahead of crack tip at the specified distance of 0.10 and 0.25mm.

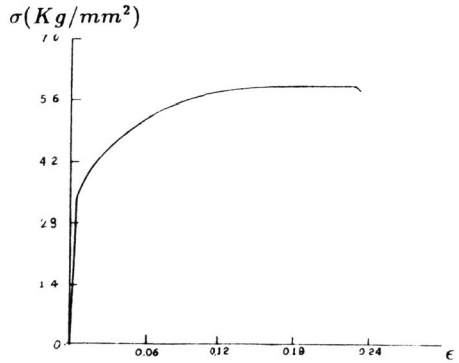

Figure 1. Stress-strain curve of 2Cr13 stainless steel.

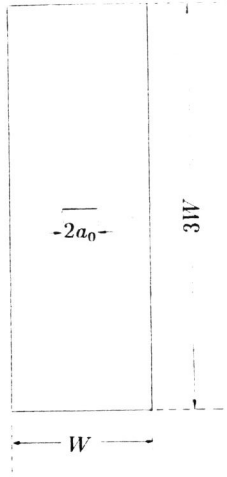

Figure 2. Center-cracked panel.

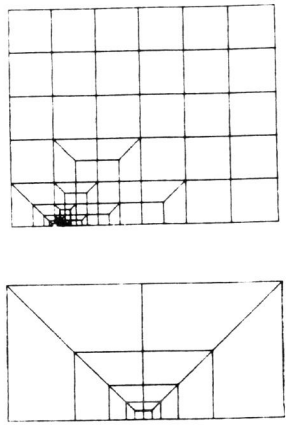

Figure 3.

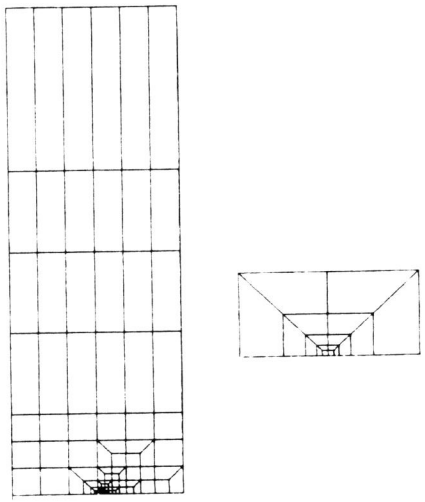

Figure 4.

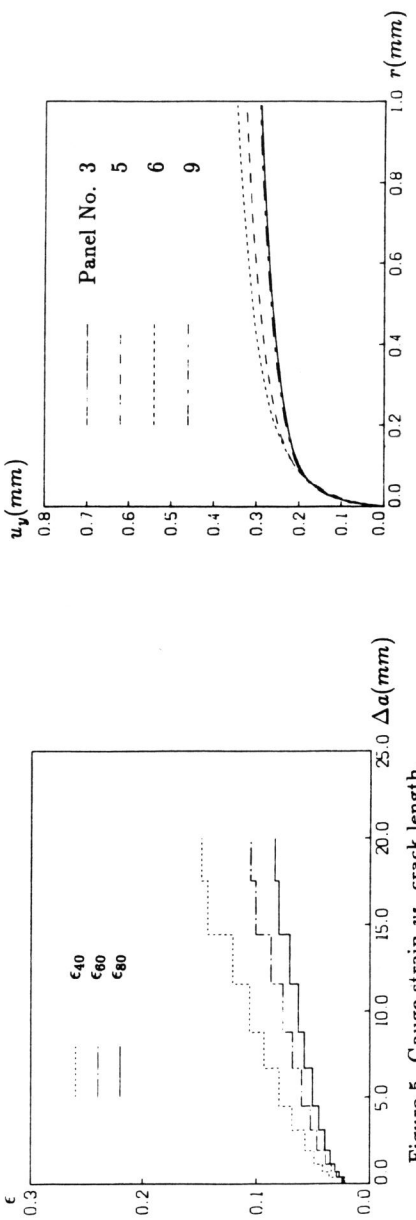

Figure 5. Gauge strain *vs.* crack length.

Figure 6. Crack shapes at crack growth initiation.

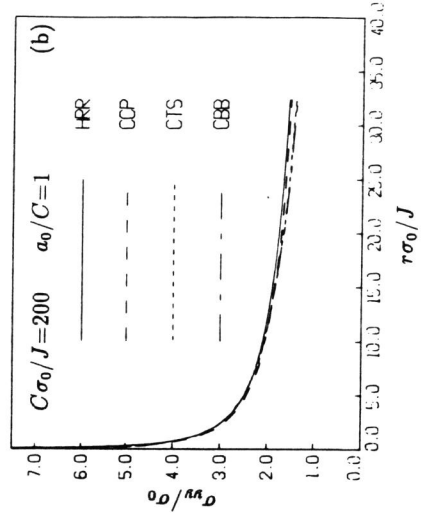

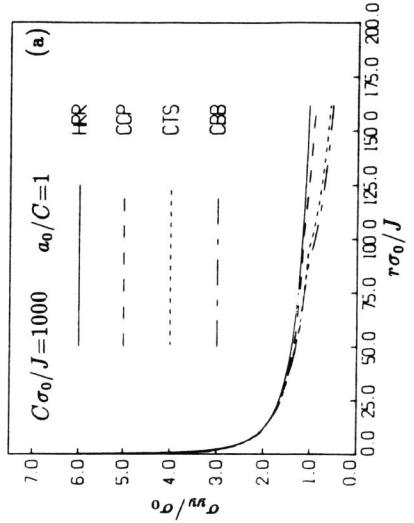

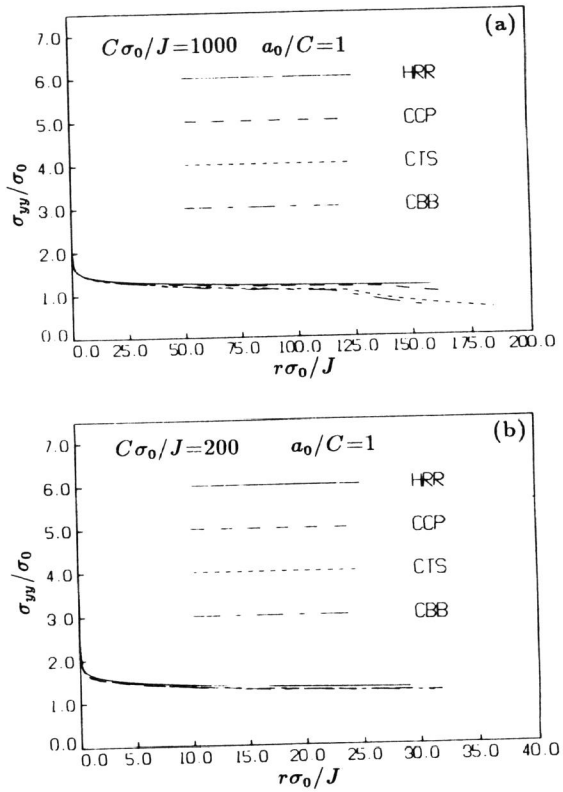

Figure 8. Stress distribution ahead of crack tip ($\theta = 0^o$)
Low hardening material n=10. C-ligament, a_0-crack length.